[CANCER RESEARCH 60, 3965–3970, July 15, 2000]

Dnmt1$^{N/+}$ Reduces the Net Growth Rate and Multiplicity of Intestinal Adenomas in C57BL/6-*Multiple Intestinal Neoplasia* (*Min*)/+ Mice Independently of *p53* but Demonstrates Strong Synergy with the *Modifier of Min 1*^{AKR} Resistance Allele[1]

Robert T. Cormier and William F. Dove[2]

McArdle Laboratory for Cancer Research [R. T. C., W. F. D.] and Laboratory of Genetics [W. F. D.], University of Wisconsin, Madison, Wisconsin 53706

ABSTRACT

Altered patterns of the 5-cytosine methylation of genomic DNA are associated with the development of a wide range of human cancers. We have studied the mechanisms and genetic pathways by which a targeted heterozygous deficiency in the murine 5-cytosine DNA methyltransferase gene (*Dnmt1*$^{N/+}$) diminishes intestinal tumorigenesis in C57BL/6-*multiple intestinal neoplasia* (*Min*)/+ mice. We found that *Dnmt1*$^{N/+}$ retards the net growth rate of intestinal adenomas and reduces tumor multiplicity by approximately 50%. This tumor resistance affects the entire intestinal tract and is independent of the status of *modifier of Min 1* and *p53*, two loci that have been found to confer strong resistance to *Min*-induced neoplasia. Interestingly, *Dnmt1*$^{N/+}$ and *modifier of Min 1* resistance interact synergistically, together virtually eliminating tumor incidence. This finding may provide an insight into potential combinatorial therapeutic approaches for treating human colon cancer.

INTRODUCTION

Altered patterns of 5-cytosine methylation at CpG islands located in the promoter region of genes are correlated with the development of a wide range of human cancers. These changes have been linked to both increases and decreases in the transcription of genes thought to be critically important for carcinogenesis. Examples of proto-oncogene activation, ostensibly via promoter hypomethylation, include *BCL-2* in B-cell leukemias (1), *MYC* and *epidermal growth factor receptor* in hepatocellular carcinomas (2, 3), Ha-*RAS* in lung cancer (4), and the biallelic expression of the imprinted *insulin-like growth factor 2* locus in Wilms' tumor (5). Alternatively, there are also numerous reports connecting gene promoter hypermethylation to the silencing of tumor suppressor genes.

Consistent with Knudson's "two-hit" hypothesis (6), such events can provide one or more inactivating hits in the development and progression of cancers. Examples include *RB* in retinoblastoma (7); *VHL* in renal carcinoma (8); *p15* in gliomas and leukemias (9); *BRCA1* in breast cancer (10); *E-CADHERIN* in hepatocellular carcinoma, breast cancer, and prostate cancer (11, 12); *GSTP1* in prostate, breast, and renal cancer (13, 14); and *p16*^{INK4a} in virtually all human cancers studied (15, 16). It remains to be determined what upstream causes generate these changes in CpG-methylation status in tumor lineages.

One of the major human cancers in the United States is colorectal cancer, accounting for 130,000 new cases and more than 50,000 deaths each year (17). It is estimated that 50% of the Western population can expect to develop at least one colorectal tumor by the age of 70 (18). Molecular analyses of human colorectal cancers have identified a growing number of cancer-linked genes, the promoters of which are differentially hypermethylated in tumors, sometimes biallelically. This list includes *p15* (19), *p16*^{INK4a} (16), *estrogen receptor* (20), *MLH1* (21–23), *WT1* (24), and *APC*[3] (25) in primary tumors and *MUC2* (26) in colon cancer cell lines. *MLH1* appears to be a special target for this silencing mechanism because this locus may be monoallelically or biallelically hypermethylated in more than 80% of the human colorectal cancers showing microsatellite instability (27).

An extremely useful tool for understanding the etiology of human cancers is a mutant mouse model. A model of intestinal cancer is the Min mouse, which carries a germ-line mutation in the *Apc* gene (note: *Min* is used as a genotypic abbreviation for *Apc*$^{Min/+}$ whenever strain genotypes are indicated, and Min is used generically for mice and tumors). On the B6 genetic background, this mutation predisposes heterozygous mice to the development of as many as 300 adenomas throughout the intestinal tract (28). *Apc* is the mouse homologue of *APC*, which has been found to be mutant in a majority of familial and sporadic human colon cancers (29). In an important study, Laird *et al.* (30) bred the Min mouse to animals carrying a targeted heterozygous deficiency in the *Dnmt1*$^{S/+}$ gene. Dnmt1 catalyzes the transfer of methyl groups from *S*-adenosyl-*L*-methionine to carbon 5 of cytosine residues in 5′-CpG-3′ dinucleotides. Maintenance methylation occurs post-DNA replication and uses the parental strand as a template, thus maintaining genomic methylation patterns (31). In the Laird *et al.* (30) study, (129/SvJ *Dnmt1*$^{S/+}$ × B6-*Min*/+) F1 progeny developed 60% fewer intestinal adenomas than F1 *Dnmt1*$^{+/+}$ *Min*/+ control animals. When global genomic methylation levels were further depressed by early administration of the pharmacological demethylating agent 5-Aza-dC, tumor incidence was reduced by a factor of nearly 60 (30).

How does a decrease in genomic methylation cause the suppression of *Min*-induced intestinal tumorigenesis? Two functions of methylation were initially considered: promotion of somatic mutagenesis by 5-methylcytosine and loss of genomic stability (30). The involvement of DNA methylation in promoting mutagenesis has been observed in bacteria, and in mammals, its importance is inferred from the low frequency of the CpG dinucleotide in the genome (32). In cancer, it has been proposed that methylated CpG residues are mutational hot spots for the generation of transition mutations caused by the deamination of 5-meC, possibly mediated by the actions of Dnmt1. Analysis of the mutational spectrum of the tumor suppressor *p53* has provided one piece of evidence for this hypothesis (33, 34). However, subsequent investigations by Chen *et al.* (35) demonstrated that hypomethylation enhanced, rather than decreased, the mutation rate at a mouse test locus. This finding is consistent with the hypothesis of Smith and Crocitto (36) that mammalian DNA methyltransferases can maintain genomic stability by preventing clastic mutagenesis. Furthermore, studies of human colon cancer cell lines by Lengauer *et al.* (37) indicate that genomic hypomethylation is likely to be associated with an increase in genomic instability. Jackson-Grusby and Jaenisch (38) also tested the effect of hypomethylation in *Min* mice fed a diet deficient in choline and methionine. *Min*-induced tumor multiplicity was reduced in mice fed the methyl group-restricted diet. Together,

Received 12/2/99; accepted 5/10/00.

The costs of publication of this article were defrayed in part by the payment of page charges. This article must therefore be hereby marked *advertisement* in accordance with 18 U.S.C. Section 1734 solely to indicate this fact.

[1] This study was supported by NIH Grants CA 07075 (to the McArdle Laboratory); CA 50585 and CA 63677 (to W. F. D.), and predoctoral training grant CA 09135 (R. T. C.).

[2] To whom requests for reprints should be addressed, at McArdle Laboratory for Cancer Research, University of Wisconsin-Madison, 1400 University Avenue, Madison, WI 53706. Phone: (608) 262-4977; Fax: (608) 262-2824; E-mail: dove@oncology.wisc.edu.

[3] The abbreviations used are: APC, adenomatous polyposis coli; B6, C57BL/6; *Mom1*, modifier of Min 1; *Min*, multiple intestinal neoplasia; BrdUrd, 5-bromodeoxyuridine; *Dnmt1*, maintenance 5-cytosine DNA methyltransferase gene; 5-Aza-dC, 5-Aza-2-deoxycytidine; PCNA, proliferating cell nuclear antigen; NSAID, nonsteroidal anti-inflammatory drug.

these studies support the hypothesis that the reduction in methylation levels, rather than the reduction in the levels of the enzyme, is the cause of intestinal tumor resistance.

To explore hypomethylation-mediated resistance to *Min*-induced tumorigenesis, we have used a mouse carrying the *N* mutant allele of *Dnmt1* (39) on an inbred B6 genetic background. The *N* allele of *Dnmt1* has a biochemical phenotype that is comparable to but slightly weaker than the *S* mutant allele of *Dnmt1* used by Laird *et al.* (30).[4] We have tested the hypothesis, first proposed by Balmain (40), that DNA methylation affects a growth regulatory gene, by examining the growth kinetics of intestinal tumors arising in B6-*Min Dnmt1*$^{N/+}$ mice. To test for independence between the effects of distinct resistance modifier loci, we have made genetic crosses to detect interactions between *Dnmt1*$^{N/+}$ and *Mom1* (40) or *p53*, two loci that confer a strong resistance to *Min*-induced neoplasia. Finally, we have assessed the potential effect of *Dnmt1*$^{N/+}$ on cellular indices of apoptosis, mitosis, and DNA synthesis in preneoplastic intestinal mucosa.

MATERIALS AND METHODS

Animal Care and Breeding. Experimental mice were bred at the McArdle Laboratory for Cancer Research. Diets and husbandry were as described previously (28).

Experimental Classes of Mice. The B6-Min pedigree has been maintained by backcrossing B6-*Apc*$^{Min/+}$ males to B6 females ($n > 40$). The B6-*Mom1*^{AKR} congenic strain has been maintained as described (41). B6-*Dnmt1*$^{N/+}$ mice were obtained from The Jackson Laboratory (Bar Harbor, ME; $n > 15$). The B6-*p53*$^{-/-}$ line originated from a (129/Sv × B6) F2 female founder that carried a targeted disruption of the *p53* gene (42). This founder was obtained from Larry Donehower (Division of Molecular Virology at Baylor University, Houston, TX). The congenic line was developed by backcrossing *p53*$^{+/-}$ females to B6 or B6-*Apc*$^{Min/+}$ males for a minimum of 10 generations.

Mice listed in Tables 1–5 and Figs. 1 and 2 were primarily generated from crosses between B6-*Apc*$^{+/+}$ *Dnmt1*$^{N/+}$ *Mom1*$^{AKR/B6}$ females × B6-*Apc*$^{Min/+}$ *Dnmt1*$^{+/+}$ *Mom1*$^{AKR/B6}$ males. Mice described in Table 6 were primarily generated from crosses between B6-*Apc*$^{+/+}$ *Dnmt1*$^{N/+}$ *p53*$^{+/-}$ females × B6-*Apc*$^{Min/+}$ *Dnmt1*$^{+/+}$ *p53*$^{-/-}$ males. Only male B6-Min *p53*$^{-/-}$ mice survived to 90 days of age, because *p53*$^{-/-}$ females are subject to several developmental abnormalities (43).[5]

Intestinal Tumor Scoring and Sizing. All mice were sacrificed by CO_2 asphyxiation. The entire intestinal tract was removed, prepared, and fixed as described previously (28). Tumors (≥0.4 mm) were scored from postfixed tissues with a Nikon SMZ-U dissecting microscope at × 10 magnification. Tumor sizes were estimated by measuring the maximum diameter of tumors from the small intestine with a calibrated eyepiece reticle. All tumors were scored by a single observer (R. T. C.) who was blind to the genotype of the sample.

Genotyping. DNA was isolated from blood as described previously (44). The *Apc* and *p53* genotypes were determined as described previously (41, 45). The genotype at the *Mom1* locus was assigned on the basis of genotypes at the closely linked flanking markers *D4Mit54* and *D4Mit13*, as described previously (41). The genotype for the *Dnmt1 N* and *Dnmt1* wild-type alleles was determined by PCR analysis using oligonucleotide primers (exon 1-1, Nae 3′, and PGKPr-1) flanking the pMT(N)neo targeting vector (39). The following primer sequences were provided by Rudi Jaenisch (Massachusetts Institute of Technology): exon 1-1, 5′-GGG CCA GTT GTG TGA CTT GG-3′; Nae 3′, 5′-CTT GGG CCT GGA TCT TGG GGA TC-3′; and PGKPr-1, 5′-GGG AAC TTC CTG ACT AGG GG-3′. PCR was carried out as follows: each DNA sample (2 μl) was amplified in a 25-μl reaction containing 2 μl of primer exon 1-1 (2 μM), 1 μl of primer Nae 3′ (2 μM), 1 μl of primer PGKPr-1 (2 μM), 1.5 μl of $MgCl_2$ (25 mM, Promega), 2.5 μl of 10× reaction buffer (Promega), 0.5 μl of dNTPs (25 mM, Promega), 0.4 μl of Taq polymerase (5 units/μl, Promega), and 14.1 μl of doubly distilled water. Samples were amplified in a PTC-200 Peltier thermal cycler (MJ Research) under the following conditions: 1 cycle at 95°C for 4 min; 25 cycles at 95°C for 1 min, 54°C for 1 min, 72°C for 1 min; 1 cycle at 72°C for 3 min; and cooling to 4°C. Agarose gel (2.0%) electrophoresis of the PCR products followed by ethidium bromide staining permits visualization of 334-bp wild-type and 472-bp *N* bands.

Histology. Tissue specimens analyzed by fixed positional analysis of intestinal crypts were isolated from the medial 4-cm section of the small intestine and the distal region of the large intestine. The intestine was cut longitudinally, rinsed in 1× PBS, fixed flat overnight in 10% formalin, washed, transferred to 70% ethanol, embedded in paraffin, and serially sectioned (5 μM), with alternate sections stained with H&E. All animals were sacrificed at approximately the same time of day to reduce the influence of circadian variation in cellular proliferation and apoptosis.

Morphological Analysis for Mitosis and Apoptosis. Quantitative analysis of apoptosis and mitosis in the intestinal crypts of histologically normal mucosa was conducted using the static positional scoring method developed by Potten *et al.* (46, 47). Briefly, 100 complete half-crypt sections per mouse were analyzed from both the medial small intestine and the distal large intestine. Samples were scored with an Olympus BX-40 System microscope at × 600 magnification by one observer (R. T. C.) who was blind to the genotype. In this method, each intestinal crypt cell position is numbered and scored for either an apoptotic or mitotic event with morphological criteria. Scores were entered into the PC-Crypts program (provided by Dr. Potten) using a laptop computer. The PC-Crypts program yields crypt mitotic and apoptotic indices and the relative distribution of these events along the crypt.

DNA Synthesis Analysis. BrdUrd (Sigma B5002) at a dose of 400 mg/kg body weight was administered by i.p. injection 40 min prior to sacrifice. Paraffinized serial sections of formalin-fixed tissues prepared for morphological analysis (described above) were processed for BrdUrd incorporation as follows. Sections were dewaxed in xylene; rehydrated through serial ethanol solutions; washed in distilled water; protease digested; blocked for endogenous peroxide, avidin, and biotin; and then incubated at room temperature with 1° BrdUrd monoclonal mouse IgG antibody (M0744, DAKO A/S, Glostrup, Denmark). After washing in 1× PBS, biotinylated 2° goat antimouse IgG antibody (Sigma B-8774) was applied, followed by a wash in 1× PBS. Samples were then treated with streptavidin peroxidase conjugate, stained with 3-amino-9-ethylcarbazole (AEC; Zymed, 00-2007) to visualize the BrdUrd antigen, and lightly counterstained with hematoxylin. Intestinal crypt cells were then scored for BrdUrd-positive staining, with the same scoring system as described above for morphological analysis.

Statistics. One-sided *P*s for tumor numbers and intestinal tumor sizes were determined by comparison of each test class with contemporaneous B6-Min control mice (often siblings) by use of the nonparametric Wilcoxon rank-sum test. One-sided *P*s for the fixed positional analysis of intestinal crypt apoptosis and proliferation were determined using Student's *t* test.

RESULTS

***Dnmt1*$^{N/+}$ Controls the Size of *Min* Adenomas.** When measured at 100 days of age, adenomas from the small intestine of B6-Min *Dnmt1*$^{N/+}$ mice are significantly smaller than those from B6-Min siblings (see Table 1). In the *Dnmt1*$^{N/+}$ class, no tumors greater than 3.8 mm were observed, whereas 17 larger adenomas were found in a comparable group of B6-Min control mice. Moreover, only 1.1% of *Dnmt1*$^{N/+}$ tumors grew to a size of 3.0 mm, whereas 7.7% of Min control tumors reached this size (see Fig. 1). This effect on intestinal adenoma size is not attributable to a shift in the distribution of tumors (see Table 2) but is strongly associated

Table 1 *Dnmt1*$^{N/+}$ *limits tumor size and acts synergistically with Mom1*^{AKR} *Dnmt1*$^{N/+}$ *and Mom1*^{AKR} *tumors were significantly smaller than controls*

Tumor sizes were measured at 100 days of age and represent the largest average diameters of adenomas from the small intestine. n = number of mice per class; all small intestinal tumors from each mouse were measured. Tumor size represents mouse averages. *P*s are highly significant, comparing B6-Min with B6-Min *Dnmt1* $^{N/+}$ ($P = 7.0 \times 10^{-7}$) or *Mom1*^{AKR} ($P = 2.3 \times 10^{-8}$) classes. Addition of *Dnmt1*$^{N/+}$ to *Mom1*$^{AKR/B6}$ reduces average maximum diameters (1.14–1.06 mm) by a degree that is close to significance ($P = 0.06$), whereas the addition of *Dnmt1*$^{N/+}$ to *Mom1*$^{AKR/AKR}$ causes a reduction in adenoma size (1.14–0.75 mm) that is highly significant ($P = 0.006$).

Class	*n*	Tumor size (mm)
B6-*Min*	35	1.56 ± 0.31
B6-*Min Dnmt1*$^{N/+}$	22	1.19 ± 0.17
B6-*Min Mom1*$^{AKR/B6}$	30	1.14 ± 0.22
B6-*Min Dnmt1*$^{N/+}$ *Mom1*$^{AKR/B6}$	22	1.06 ± 0.38
B6-*Min Mom1*$^{AKR/AKR}$	6	1.14 ± 0.30
B6-*Min Dnmt1*$^{N/+}$ *Mom1*$^{AKR/AKR}$	11	0.75 ± 0.28

[4] R. Jaenisch, personal communication.
[5] R. Halberg, unpublished observations.

with inhibition of the net growth rate of individual adenomas (see Table 1 and Fig. 2). We restricted our analysis to adenomas of the small intestine because of low tumor multiplicities in the large intestine and the difficulty in accurately measuring the diameters of pedunculated colonic adenomas. However, it appears that *Dnmt1*$^{N/+}$ also restricts adenoma growth in the large intestine.

***Dnmt1*$^{N/+}$ Significantly Retards the Net Growth Rate of *Min* Adenomas.** To determine whether the reduction in the size of B6-Min *Dnmt1*$^{N/+}$ adenomas was caused by a slowing in the net tumor growth rate, the tumor sizes were scored at 70, 100, and 130 days (see Fig. 2). We found that B6-Min *Dnmt1*$^{N/+}$ and B6-Min control tumors were similar in size at 70 days of age but diverged soon after. Linear regression analysis of maximum tumor diameters demonstrated a 2.5-fold higher rate of increase in tumor diameters in Min control mice than in *Dnmt1*$^{N/+}$ carriers. Because it was difficult to obtain many B6-Min control mice that lived to 130 days, we used a 120-day time point for controls. At 120 days, tumors from control mice were significantly larger than adenomas obtained from B6-Min *Dnmt1*$^{N/+}$ mice measured at 130 days.

***Dnmt1*$^{N/+}$ and *Mom1*^{AKR} Act Synergistically.** On the B6 genetic background, heterozygosity for the *N* allele of *Dnmt1* reduces *Min*-induced intestinal tumorigenesis by a factor of 2 (Table 3). A similar effect has been observed in congenic mice that are heterozygous for the *Mom1* AKR-derived region of distal chromosome 4 (44). To test for a genetic interaction between *Dnmt1*$^{N/+}$ and *Mom1*^{AKR}, we scored intestinal tumors from mice resulting from crosses as described in "Materials and Methods." Heterozygosity for either the *N* allele of *Dnmt1* or the *Mom1*^{AKR} resistance allele reduced tumor multiplicity by a factor of 2. *Mom1* had previously been shown to act in a semi-dominant fashion (44). Mice homozygous for *Mom1*^{AKR} demonstrated a reduction in tumor multiplicity by a factor of 5, a phenotype similar to that observed in *Dnmt1*$^{N/+}$ *Mom1*$^{AKR/B6}$ double heterozygotes. A more striking effect was observed when *Mom1* was homozygous for the AKR resistance allele. *Dnmt1*$^{N/+}$ *Mom1*$^{AKR/AKR}$ mice developed fewer tumors by a factor of 44 (Table 3), with almost half exhibiting no intestinal tumors. Furthermore, the few adenomas observed tended to be very small (Table 1).

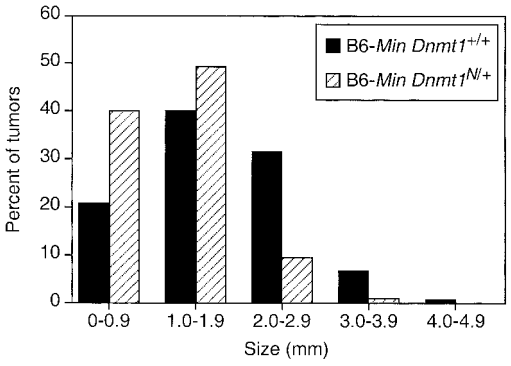

Fig. 1. The *Dnmt1*$^{N/+}$ class of Min tumors was deficient for larger adenomas in the small intestine. This histogram represents ~600 tumors pooled from each genotype. Size is the maximum diameter of adenomas.

Table 2 *Effect of Dnmt1*$^{N/+}$ *and Mom1*^{AKR} *on tumor distribution Dnmt1*$^{N/+}$ *influenced tumorigenesis throughout the intestinal tract*

Representative 4-cm sections were scored from the small intestine, with the proximal section beginning at the pyloric junction and the most distal section taken next to the ileo-cecal junction. The entire colon was scored in this analysis. Tumor sizes were measured at 100 days of age and represent the largest average diameters. *n*, number of mice; SI, small intestine.

		Mean tumor count/mean tumor size (mm)			
Class	*n*	Proximal SI	Medial SI	Distal SI	Colon
B6-*Min*	36	5.0/(2.26)	9.9/(1.69)	8.0/(1.80)	2.7/(3.95)
B6-*Min Dnmt1*$^{N/+}$	23	1.7/(2.08)	3.7/(1.41)	3.8/(1.14)	1.8/(3.19)
B6-*Min Mom1*$^{AKR/B6}$	29	2.8/(1.81)	5.8/(1.27)	3.7/(0.85)	1.0/(3.59)

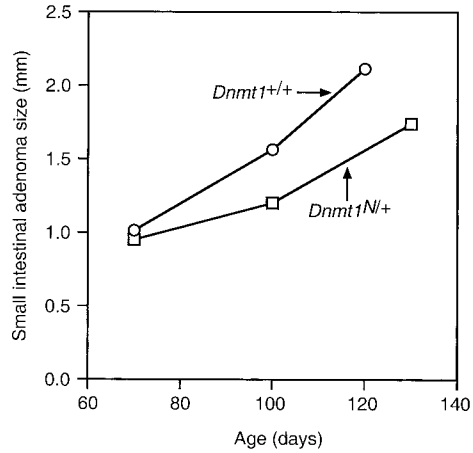

Fig. 2. *Dnmt1*$^{N/+}$ retarded the net tumor growth rate of *Min*-induced adenomas in the small intestine. Tumor sizes were plotted at 70, 100, and 130 days of age. Tumor sizes were not significantly different at 70 days, but became significantly different at 100 days and beyond. Because of early mortality of the B6-Min *Dnmt1*$^{+/+}$ class, size could be plotted only at 120 days, but this value was significantly greater than B6-Min *Dnmt1*$^{N/+}$ tumors measured at 130 days; $P < 0$ .05. Tumor sizes represent per-mouse averages. The numbers of mice measured were as follows. 70 days: Min control, $n = 5$; *Dnmt1*$^{N/+}$, $n = 5$. 100 days: Min control, $n = 36$; *Dnmt1*$^{N/+}$, $n = 23$. 120 days: Min control, $n = 13$. 130 days: *Dnmt1*$^{N/+}$, $n = 17$. Min controls measured at 110 days (1.95 mm; not indicated on graph) were also larger than *Dnmt1*$^{N/+}$ tumors measured at 130 days (1.70 mm).

Table 3 *Synergy between Dnmt1*$^{N/+}$ *and Mom1*^{AKR} *on tumor multiplicity Dnmt1*$^{N/+}$ *strongly reduced intestinal tumor multiplicity independently of Mom1*

Crosses between B6-*Apc*$^{+/+}$ *Dnmt1*$^{N/+}$ *Mom1*$^{AKR/B6}$ females × B6-Min *Dnmt1*$^{N/+}$ *Mom1*$^{AKR/B6}$ males yielded six informative classes of Min offspring. Animals were sacrificed at 100 days of age, and their entire intestinal tracts were scored for adenomas. $P < 0.05$, comparing B6-Min control mice with all other classes. $P < 0.05$, comparing B6-Min *Dnmt1*$^{N/+}$ *Mom1*$^{AKR/AKR}$ class with all other classes.

	No. of tumors (mean ± SD)	
	Dnmt1$^{N/+}$	*Dnmt1*$^{+/+}$
Mom1$^{B6/B6}$	41 ± 15	88 ± 30
Mom1$^{AKR/B6}$	13 ± 9	44 ± 21
Mom1$^{AKR/AKR}$	2 ± 2	16 ± 7

Dnmt1$^{N/+}$ and *Mom1*^{AKR} also demonstrate additivity in reducing adenoma size (Table 1). Tumors from *Dnmt1*$^{N/+}$ *Mom1*$^{AKR/B6}$ mice (1.06 mm) are smaller than tumors from either *Dnmt1*$^{N/+}$ (1.19 mm) or *Mom1*$^{AKR/B6}$ (1.14 mm) by a degree that is significant for *Dnmt1*$^{N/+}$ alone ($P = 0.004$) and that is close to significant for *Mom1*$^{AKR/B6}$ alone ($P = 0.06$), whereas tumors from *Dnmt1*$^{N/+}$ *Mom1*$^{AKR/AKR}$ mice (0.75 mm) are strikingly smaller than adenomas obtained from *Mom1*$^{AKR/AKR}$ mice (1.14 mm; $P = 0.006$).

***Dnmt1*$^{N/+}$ Suppresses Tumorigenesis throughout the Intestinal Tract.** Recent studies by our group indicate that the B6 intestine consists of discrete subregions that are differentially susceptible to *Min*-induced tumorigenesis. Modifiers of *Min* can act differentially in various parts of the intestinal tract.[6, 7] Furthermore, in several mouse models of intestinal cancer, such as genetic knockouts in the *Tgf-β* pathway, neoplasia is restricted to the large intestine (48). Here, we report that *Dnmt1*$^{N/+}$ provides tumor resistance in all regions of the intestine, with the strongest effect in the proximal half of the small intestine (see Table 2) and a more modest effect in the large intestine. By contrast, *Mom1*^{AKR} exerts its strongest effect in both the distal half of the small intestine and the large intestine.

***Dnmt1* Deficiency Does Not Alter Apoptotic Indices in the Intestinal Crypt and May Help Restore Rates of Proliferation.** To define further the mode of action of *Dnmt1*$^{N/+}$, we measured the

[6] A. Bilger, personal communication.

[7] R. Cormier, A. Bilger, A. Lillich, R. Halberg, K. Hong, K. Gould, N. Borenstein, E. Lander, and W. Dove. The *Mom1*^{AKR} intestinal tumor resistance region consists of *pla2g2a* and a locus distal to *D4Mit64*, submitted for publication.

Table 4 *Effect of Dnmt1*$^{N/+}$ *on mitotic and apoptotic indices Dnmt1*$^{N/+}$ *had no significant effect on apoptotic or mitotic indices in preneoplastic intestinal crypts but may act to normalize rates of mitosis*

H&E sections were scored by morphological criteria for apoptosis and mitosis. Each sample group represents ~20,000 cells scored/class (from 10 animals) in each category. Indices represent averages of per-animal frequencies. All scoring was conducted by one investigator blind to the genotype of the sample. $P < 0.05$ for mitotic indices comparing B7-*Apc*$^{+/+}$ and B6-Min classes. All other comparisons were not significantly different.

Class	Apoptotic index (mean ± SD)		Mitotic index (mean ± SD)	
	Small intestine	Colon	Small intestine	Colon
B6-*Apc*$^{+/+}$	0.50 ± 0.38	0.38 ± 0.19	4.17 ± 1.6	1.39 ± 0.53
B6-*Min*	0.37 ± 0.25	0.18 ± 0.16	2.49 ± 0.52	1.05 ± 0.41
B6-*Min Dnmt1*$^{N/+}$	0.31 ± 0.14	0.22 ± 0.12	2.78 ± 0.46	1.28 ± 0.45

Table 5 *Effect of Dnmt1*$^{N/+}$ *and Mom1*^{AKR} *on BrdUrd labeling indices Dnmt1*$^{N/+}$ *and Mom1*^{AKR} *reversed Min-induced depression of BrdUrd-labeling indices*

Serial sections of intestinal crypts analyzed morphologically for apoptosis and mitosis were scored for incorporation of BrdUrd during S-phase of the cell cycle. Each class represents ~20,000 cells (from 10 animals of each genotype). Indices are the number of events (*e.g.*, mitotic figures, apoptotic cells, BrdUrd-labeled cells) divided by the number of cells scored in the assay times 100 and represent averages of per-animal indices. $P < 0.05$, comparing B6-Min class with each modifier class. To eliminate potential batch variation in BrdUrd staining intensity, all samples were stained in one tray for an identical period of time. An age-matched B6-*Apc*$^{+/+}$ class was excluded from this analysis because it was not stained for BrdUrd in the same batch as the B6-Min samples.

Class	Labeling index (mean ± SD)	
	Small intestine	Colon
B6-*Min*	23.5 ± 3.8	9.1 ± 4.0
B6-*Min Dnmt1*$^{N/+}$	28.0 ± 2.6	10.5 ± 2.8
B6-*Min Mom1*$^{AKR/B6}$	28.3 ± 2.5	11.2 ± 3.6
B6-*Min Dnmt1*$^{N/+}$ *Mom1*$^{AKR/B6}$	27.5 ± 2.8	10.7 ± 2.2
B6-*Min Mom1*$^{AKR/AKR}$	28.0 ± 2.5	11.8 ± 3.1
B6-*Min Dnmt1*$^{N/+}$ *Mom1*$^{AKR/AKR}$	28.0 ± 2.5	9.7 ± 2.8

apoptotic, mitotic and BrdUrd labeling indices in histologically normal crypts of B6-*Apc*$^{+/+}$, B6-Min, B6-Min *Dnmt1*$^{N/+}$, and Min mice heterozygous or homozygous for the *Mom1* AKR allele (Tables 4 and 5). *Dnmt1*$^{N/+}$ had no significant impact on the apoptotic index and, instead, appears to elevate the mitotic and BrdUrd labeling indices *versus* B6-Min controls. The difference is statistically significant only in the BrdUrd labeling indices ($P < 0.05$); however, the *Min* mutation itself led to a significant systemic reduction in DNA synthesis compared with the marginal effects of both *Dnmt1*$^{N/+}$ and *Mom1*^{AKR}. Notably, B6-Min control animals also had significantly reduced mitotic indices ($P < 0.05$) compared with B6-*Apc* wild-type mice.

***Dnmt1*$^{N/+}$'s Tumor Resistance Does Not Require a Functional Allele of *p53*.** *p53* has been found to be inactivated in more than 50% of all human cancers, including colorectal adenocarcinoma (49). One particular hypothesis predicts that the *Dnmt*$^{N/+}$ effect depends on p53 function, *e.g.*, possibly via an apoptotic mechanism. To test for interaction between *Dnmt1*$^{N/+}$ and *p53*, we crossed *Dnmt1*$^{N/+}$ into a congenic B6-Min *p53*$^{-/-}$ line developed from a targeted knockout of *p53* provided by L. Donehower (42). Nullizygosity for *p53* enhances both the multiplicity and progression of B6-Min tumors (50). We have confirmed that complete loss of *p53* function significantly increases *Min*-induced tumor multiplicity and may also significantly increase adenoma size in regions of the small intestine. However, in the absence of *p53*, *Dnmt1*$^{N/+}$ exerted a strong resistance to tumor incidence and continued to have a significant effect on adenoma size (Table 6). These effects were observed throughout the intestinal tract (data not shown).

DISCUSSION

It is now well known that accumulated genetic and epigenetic alterations accompany neoplastic development in many human tissues. In the colon, changes in the expression of *APC*, *p53*, *Ras*, and *β-Catenin*, (and surely other genes) are observed during the progressive transformation of normal mucosal tissue to adenomas and eventually malignant carcinomas. In this study, we used the *Dnmt1*$^{N/+}$ mutant mouse to extend the important work of Laird *et al.* (30) by addressing some of the functional mechanisms and genetic pathways by which *Dnmt1*$^{N/+}$ provides resistance to *Min*-induced tumorigenesis. Use of the *N* knockout allele of *Dnmt1* permits an assessment of the *Dnmt1* heterozygous knockout phenotype on a homogeneous B6 background, alone and in combination with *Mom1*^{AKR} and *p53*-deficiency, to determine their possible interactions.

We found that *Dnmt1*$^{N/+}$ slows the rate of growth of intestinal adenomas. Tumors from the small intestine of Min *Dnmt1*$^{N/+}$ animals and their Min control siblings were similar in size at 70 days of age, but their respective growth rates diverged significantly thereafter. This result is consistent with a model in which gene promoter hypermethylation may contribute to the epigenetic silencing of a locus that negatively regulates tumor growth. Reduction in global methylation levels by a germ-line deficiency in the maintenance 5-cytosine methylase (or by administration of 5-Aza-dC to neonates) could, therefore, attenuate such modulation of a negative tumor regulator.

An alternative mechanistic explanation might involve the hypothesized interaction between Dnmt1, PCNA, and p21^{WAF1}. In a model proposed by Chuang *et al.* (51), Dnmt1 affects the cell cycle by competing with p21^{WAF1} for PCNA binding sites, and Fournel *et al.* (52) have recently reported that down-regulation of human *DNMT1* via antisense RNA induces p21^{WAF1} protein activity in cultured human tumor cells. *p21*$^{-/-}$ mice do not spontaneously develop cancer (53), but sensitization via crosses to Min might be a means to test for interaction between deficiencies in *Dnmt1* and *p21* in tumorigenesis. Nullizygosity for *p53*, a key transactivator of *p21* (54), does significantly enhance Min tumorigenesis, but *Dnmt1*$^{N/+}$ can still exert considerable tumor resistance in the absence of *p53*. This observation argues against the interaction of Dnmt1 with p21^{WAF1} and PCNA as being involved in its effect on Min tumor formation.

The tumor resistance of *Dnmt1*$^{N/+}$ is also expressed independently of the resistance allele of *Mom1*. The combined quantitative resistance phenotypes of *Dnmt1*$^{N/+}$ and *Mom1*$^{AKR/AKR}$ are far more than additive, and each resistance modifier can act in the genetic absence of the other factor. Specifically, *Dnmt1*$^{N/+}$ does not require the secreted phospholipase encoded by *Pla2g2a*, a gene that is a strong candidate for at least one component of *Mom1* (55) and that is defective in sensitive B6 mice. Regional differences in the resistance phenotypes of *Dnmt1*$^{N/+}$ and

Table 6 *Dnmt1*$^{N/+}$ *suppresses Min intestinal tumorigenesis independently of p53 Dnmt1*$^{N/+}$*'s tumor resistance did not require a functional allele of p53*

B6-*Apc*$^{+/+}$ *Dnmt1*$^{N/+}$ *p53*$^{+/-}$ females were crossed to B6-Min *Dnmt1*$^{+/+}$ *p53*$^{-/-}$ males. Experimental mice were sacrificed at 90 days of age, and adenomas were scored and sized from the entire intestinal tract. Tumor sizes in this table represent the largest average diameter (mm) in the small intestine. $P < 0.05$ for differences in mean intestinal tumor multiplicity and adenoma size. *n*, number of mice.

Class	*n*	No. of tumors (mean ± SD)		Tumor size (mm) small intestine
		Total	Colon	
B6-*Min Dnmt1*$^{+/+}$ *p53*$^{-/-}$	42	165 ± 63	6.9 ± 4.5	1.51 ± 0.16
B6-*Min Dnmt1*$^{N/+}$ *p53*$^{-/-}$	35	93 ± 33	3.8 ± 3.6	1.15 ± 0.12

Mom1^{AKR} also support their action via independent pathways (Table 2). In the colon, *Dnmt1*$^{N/+}$ has a very modest effect on tumorigenesis, whereas mice overexpressing a wild-type *Pla2g2a*^{AKR} transgene on the B6 background develop 3-fold fewer colon adenomas (55). Interestingly, the combination of *Mom1*$^{AKR/AKR}$ and *Dnmt1*$^{N/+}$ demonstrated a very strong synergy, virtually abrogating tumorigenesis, with half of these mice developing no tumors at all. *Mom1*^{AKR} has previously been shown to retard net adenoma growth rate (44). Notably, the combination of *Mom1*^{AKR} and *Dnmt1*$^{N/+}$ further reduced adenoma size significantly. Thus together, *Dnmt1*$^{N/+}$ and *Mom1*$^{AKR/AKR}$ significantly reduce both the growth rate and incidence of *Min*-induced tumors, suggesting the potential efficacy of combinatorial therapeutic protocols based on their distinct biochemical activities.

The preliminary result that *Dnmt1*$^{N/+}$ does not alter apoptotic indices in histologically normal intestinal mucosa of the Min mouse nominally distinguishes the biochemical mode of action of *Dnmt1*$^{N/+}$ from some other known classes of intestinal anticancer agents, such as the NSAIDs (56). The ability of NSAIDs to cause intestinal tumor regression has been linked to their effect on rates of apoptosis in both normal mucosa and in tumors (57). The finding that *Dnmt1*$^{N/+}$ and *Mom1*^{AKR} may act to normalize rates of proliferation in non-tumor-bearing crypts requires further investigation. We observed that Min animals have reduced indices of mitosis and DNA synthesis in histologically normal crypts. This effect does not result from an increase in crypt length (data not shown). Both *Dnmt1*$^{N+}$ and *Mom1*^{AKR} appear to reverse partially this reduction in crypt cell proliferation, although the difference is significant only for the BrdUrd labeling index. Mahmoud *et al.* (57–59) have reported that *Min* significantly decreases the PCNA-labeling index and slows the migration rate of enterocytes in normal intestinal tissue. They have also reported that NSAIDs, such as sulindac, can restore both cellular proliferation and enterocyte migration rates to wild-type levels (58). Investigators in our laboratory have long observed that nonneoplastic crypts and villi surrounding Min adenomas are decidedly hyperplastic, but our current results and those of the Bertagnolli group indicate that this hyperplasia probably does not involve increased DNA synthesis rates. We are currently investigating whether *Dnmt1*$^{N/+}$ can modulate the maturation of migrating enterocytes within the intestinal crypt. A failure of *APC* mutant cells to differentiate properly has been observed previously in human familial adenomatous polyposis patients (60), an observation that correlates with the development of preneoplastic dysplastic lesions and adenomas. In addition, Wasan *et al.* (61) have proposed that familial adenomatous polyposis patients have a deficiency in intestinal crypt differentiation, specifically through the crypt cycle. Differential methylation has been shown to be connected to the differentiation of certain mammalian cell types (62, 63), and Bestor *et al.* (64) have shown that hypomethylation can revert the phenotype of transformed mouse cells by induction of terminal differentiation.

Very little is known about how heritable, tissue-specific methylation patterns are established during development (65), let alone how regulated methylation might help to maintain adult tissue homeostasis in the rapidly renewing intestine, where cellular production, differentiation, and death are tightly controlled. As suggested by our study of tumor growth kinetics, if promoter silencing of growth-regulatory loci is important for *Min* tumorigenesis, a key question to be addressed is whether these epigenetic events occur during or prior to the clonal expansion of initiated tumor cells. This change might arise by a random embryonic *de novo* methylase activity in the pluripotent long-lived intestinal stem cells, or, as recently reported by Ramchandani *et al.* (66) and Kanai *et al.* (67) as a result of a demethylase activity.

Observations from the Jaenisch laboratory and our laboratory support the view that most *Min* intestinal tumors arise very early. In the study of Laird *et al.* (30), prevention of tumorigenesis by administration of 5-Aza-dC was efficacious only when administered early, and Shoemaker *et al.* (68) demonstrated that tumor enhancement resulting from somatic mutagenesis was optimal prior to 14 days of age. An intriguing possibility is that in Min mice a distinct subset of intestinal stem cells might demonstrate what Toyota *et al.* (69) have referred to as a "CpG island methylator phenotype," possibly formed *in utero*. Interestingly, De Marzo *et al.* (70) have recently reported that human adenomatous polyps demonstrate a striking heterogeneity in Dnmt1 protein expression, and Eads *et al.* (71) have recently found that specific CpG island hypermethylation observed in colon cancer does not correlate with the temporal overexpression of Dnmt1.

In summary, we have found that a germ-line deficiency in maintenance 5-cytosine methylation slows Min intestinal adenoma growth rate and reduces tumor multiplicity in B6 mice while also demonstrating a strong synergy with the *Mom1*^{AKR} resistance allele. These results are consistent with the selection in intestinal tumors for random differential methylation events, occurring either developmentally or in clonal tumor cell growth. Studies with the Min mouse should continue to reveal some of the underlying biology governing regulation of genomic methylation in intestinal cancer.

ACKNOWLEDGMENTS

We thank Cheri Pasch and Natalie Borenstein for the PCR genotyping; Harlene Edwards and Jane Weeks for preparation of tissue samples for histological analysis; Linda Clipson for assistance in the production of the manuscript; Ilse Riegel for review of the manuscript; Kim Severson, Matt Wiluth, and Jesse Waggoner for DNA isolation; and Jen Triemstra and the McArdle animal care staff for help in animal husbandry. In addition, we thank Rudolph Jaenisch and Peter Laird for early consultation on the *Dnmt*$^{N/+}$ phenotype, Michael Newton for his statistical analysis of the fixed positional crypt survey, Chris Potten and Anita Merritt for their advice on the positional scoring of intestinal crypts and the use of the PC-Crypts software, Richard Halberg for his general advice on the genetic interactions between *Min* and *p53*, and Larry Donehower for his generous gift of the *p53* knockout mouse. Alexandra Shedlovsky, Richard Halberg, and Kevin Haigis provided valuable critiques of the manuscript.

REFERENCES

1. Hanada, M., Delia, D., Aiello, A., Stadtmauer, E., and Reed, J. C. *bcl-2* gene hypomethylation and high-level expression in B-cell chronic lymphocytic leukemia. Blood, *82:* 1820–1828, 1993.
2. Kaneko, Y., Shibuya, M., Nakayama, T., Hayashida, N., Toda, G., Endo. Y., Oka, H., and Oda, T. Hypomethylation of *c-myc* and epidermal growth factor receptor genes in human hepatocellular carcinoma and fetal liver. Jpn. J. Cancer Res., *76:* 1136–1140, 1985.
3. Nambu, S., Inoue, K., and Sasaki, H. Site-specific hypomethylation of the c-*myc* oncogene in human hepatocellular carcinoma. Jpn. J. Cancer Res., *78:* 695–704, 1987.
4. Feinberg, A. P., and Vogelstein, B. Hypomethylation of *ras* oncogenes in primary human cancers. Biochem. Biophys. Res. Commun., *111:* 47–54, 1983.
5. Ogawa, O., Eccles, M. R., Szeto, J., McNoe, L. A., Yun, K., Maw, M. A., Smith, P. J., and Reeve, A. E. Relaxation of insulin-like growth factor II gene imprinting implicated in Wilms tumor. Curr. Biol., *5:* 1013–1016, 1995.
6. Knudson, A. G. Mutation and cancer: statistical study of retinoblastoma. Proc. Natl. Acad. Sci. USA, *68:* 820–823, 1971.
7. Ohtani-Fujita, N., Fujita, T., Aoike, A., Osifchin, N. E., Robbins, P. D., and Sakai, T. CpG methylation inactivates the promoter activity of the human retinoblastoma tumor-suppressor gene. Oncogene, *8:* 1063–1067, 1993.
8. Herman, J. G., Latif, F., Weng, Y., Lerman, M. I., Zbar, B., Liu, S., Samid, D., Duan, D-H. R., Gnarra, J. R., Linehan, W. M., and Baylin, S. B. Silencing of the *VHL* tumor-suppressor gene by DNA methylation in renal carcinoma. Proc. Natl. Acad. Sci. USA, *91:* 9700–9704, 1994.
9. Herman, J. G., Jen, J., Merlo, A., and Baylin, S. B. Hypermethylation-associated inactivation indicates a tumor suppressor role for *p15*^{INK4b}. Cancer Res., *56:* 722–727, 1996.
10. Mancini, D. N., Rodenhiser, D. I., Ainsworth, P. J., O'Malley, F. P., Singh, S. M., Xing, W., and Archer, T. K. CpG methylation within the 5′ regulatory region of the *BRCA1* gene is tumor specific and includes a putative CREB binding site. Oncogene, *16:* 1161–1169, 1998.
11. Graff, J. R., Herman, J. G., Lapidus, R. G., Chopra, H., Xu, R., Jarrad, D. F., Isaacs, W. B., Pitha, P. M., Davidson, N. E., and Baylin, S. B. E-cadherin expression is silenced by DNA hypermethylation in human breast and prostate carcinomas. Cancer Res., *55:* 5195–5199, 1995.
12. Kanai, Y., Ushijima, S., Hui, A-M., Ochiai, A., Tsuda, H., Sakamoto, M., and Hirohashi, S. The E-cadherin gene is silenced by CpG methylation in human hepatocellular carcinomas. Int. J. Cancer, *71:* 355–359, 1997.
13. Lee, W-H., Morton, R. A., Epstein, J. I., Brooks, J. D., Campbell, P. A., Bova, G. S., Hsieh, W-S., Isaacs, W. B., and Nelson, W. G. Cytidine methylation of regulatory

sequences near the π-class glutathione *S*-transferase gene accompanies human prostatic carcinogenesis. Proc. Natl. Acad. Sci. USA, *91:* 11733–11737, 1994.
14. Esteller, M., Corn, P. G., Urena, J. M., Gabrielson, E., Baylin, S. B., and Herman, J. G. Inactivation of glutathione *S*-transferase *P1* gene by promoter hypermethylation in human neoplasia. Cancer Res., *58:* 4515–4518, 1998.
15. Myohanen, S. K., Baylin, S. B., and Herman, J. G. Hypermethylation can selectively silence individual *p16*^{INK4a} alleles in neoplasia. Cancer Res., *58:* 591–593, 1998.
16. Herman, J. G., Merlo, A., Mao, L., Lapidus, R. G., Issa, J-P. J., Davidson, N. E., Sidransky, D., and Baylin, S. B. Inactivation of the *CDKN2/p16/MTS1* gene is frequently associated with aberrant DNA methylation in all common human cancers. Cancer Res., *55:* 4525–4530, 1995.
17. Cancer Facts & Figures 2000, p. 4. Atlanta, GA: American Cancer Society, 2000.
18. Kinzler, K., and Vogelstein, B. Lessons from hereditary colorectal cancer. Cell, *87:* 159–170, 1996.
19. Herman, J. G., Jen, J., Merlo, A., and Baylin, S. B. Hypermethylation-associated inactivation indicates a tumor suppressor role for *p15*^{INK4b}. Cancer Res., *56:* 722–727, 1996.
20. Issa, J-P., Ottaviano, Y. L., Celano, P., Hamliton, S. R., Davidson, N. E., and Baylin, S. B. Methylation of the oestrogen receptor CpG island links ageing and neoplasia in human colon. Nat. Genet., *7:* 536–540, 1994.
21. Benachenhou, N., Guiral, S., Gorska-Flipot, I., Michalski, R., Labuda, D., and Sinnett, D. Allelic losses and DNA methylation at DNA mismatch repair loci in sporadic colorectal cancer. Carcinogenesis (Lond.), *19:* 1925–1929, 1998.
22. Cunningham, J. M., Christensen, E. R., Tester, D. J., Kim, C-Y., Roche, P. C., Burgart, L. J., and Thibodeau, S. N. Hypermethylation of the *hMLH1* promoter in colon cancer with microsatellite instability. Cancer Res., *58:* 3455–3460, 1998.
23. Veigl, M. L., Kasturi, L., Olechnowicz, J., Ma, A., Lutterbaugh, J. D., Periyasamy, S., Li, G-M., Drummond, J., Modrich, P. L., Sedwick, W. D., and Markowitz, S. D. Biallelic inactivation of *hMLH1* by epigenetic silencing, a novel mechanism causing human MSI cancers. Proc. Natl. Acad. Sci. USA, *95:* 8698–8702, 1998.
24. Hiltunen, M. O., Koistinaho, J., Alhonen, L., Myohanen, S., Marin, S., Kosma, V-M., Paakkonen, M., and Janne, J. Hypermethylation of the *WT1* and calcitonin gene promoter regions at chromosome 11p in human colorectal cancer. Br. J. Cancer, *76:* 1124–1130, 1997.
25. Hiltunen, M. O., Alhonen, L., Koistinaho, J., Myohanen, S., Paakkonen, M., Marin, S., Kosma, V-M., and Janne, J. Hypermethylation of the *APC* (adenomatous polyposis coli) gene promoter region in human colorectal carcinoma. Int. J. Cancer, *70:* 644–648, 1997.
26. Hanski, C., Riede, E., Gratchev, A., Foss, H. D., Bohm, C., Klubmann, E., Hummel, M., Mann, B., Buhr, H. J., Stein, H., Kim, Y. S., Gum, J., and Riecken, E. O. MUC2 gene suppression in human colorectal carcinomas and their metastases: in vitro evidence of the modulatory role of DNA methylation. Lab. Invest., *77:* 685–695, 1997.
27. Herman, J. G., Umar, A., Polyak, K., Graff, J., Ahuja, N., Issa, J-P. J., Markowitz, S., Willson, J. K. V., Hamilton, S. R., Kinzler, K. W., Kane, M. F., Kolodner, R. D., Vogelstein, B., Kunkel, T. A., and Baylin, S. B. Incidence and functional consequences of *hMLH1* promoter hypermethylation in colorectal carcinoma. Proc. Natl. Acad. Sci. USA, *95:* 6870–6875, 1998.
28. Moser, A. R., Pitot, H. C., and Dove, W. F. A dominant mutation that predisposes to multiple intestinal neoplasia in the mouse. Science (Washington DC), *247:* 322–324, 1990.
29. Powell, S. M., Zilz, N., Beazer-Barclay, Y., Bryan, T. M., Hamilton, S. R., Thibodeau, S. N., Vogelstein, B., and Kinzler, K. W. *APC* mutations occur early during colorectal tumorigenesis. Nature (Lond.), *359:* 235–237, 1992.
30. Laird, P. W., Jackson-Grusby, L., Fazeli, A., Dickinson, S. L., Jung, E. W., Li, E., Weinberg, R. A., and Jaenisch, R. Suppression of intestinal neoplasia by DNA hypomethylation. Cell, *81:* 197–205, 1995.
31. Bestor, T., Laudano, A., Mattaliano, R., and Ingram, V. Cloning and sequencing of a cDNA encoding DNA methyltransferase of mouse cells. The carboxyl-terminal domain of the mammalian enzymes is related to bacterial restriction methyltransferases. J. Mol. Biol., *203:* 971–983, 1988.
32. Gonzalgo, M. L., and Jones, P. A. Mutagenic and epigenetic effects of DNA methylation. Mutat. Res., *386:* 107–118, 1997.
33. Denissenko, M. F., Chen, J. X., Tang, M-S., and Pfeifer, G. P. Cytosine methylation determines hot spots of DNA damage in the human *p53* gene. Proc. Natl. Acad. Sci. USA, *94:* 3893–3898, 1997.
34. Greenblatt, M. S., Bennett, W. P., Hollstein, M., and Harris, C. C. Mutations in the *p53* tumor suppressor gene: clues to cancer etiology and molecular pathogenesis. Cancer Res., *54:* 4855–4878, 1994.
35. Chen, R. Z., Pettersson, U., Beard, C., Jackson-Grusby, L., and Jaenisch, R. DNA hypomethylation leads to elevated mutation rates. Nature (Lond.), *395:* 89–93, 1998.
36. Smith, S. S., and Crocitto, L. DNA methylation in eukaryotic chromosome stability revisited: DNA methyltransferase in the management of DNA conformation space. Mol. Carcinog., *26:* 1–9, 1999.
37. Lengauer, C., Kinzler, K. W., and Vogelstein, B. DNA methylation and genetic instability in colorectal cancer cells. Proc. Natl. Acad. Sci. USA, *94:* 2545–2550, 1997.
38. Jackson-Grusby, L., and Jaenisch, R. Experimental manipulation of genomic methylation. Semin. Cancer Biol., *7:* 261–268, 1996.
39. Li, E., Bestor, T. H., and Jaenisch, R. Targeted mutation of the DNA methyltransferase gene results in embryonic lethality. Cell, *69:* 915–926, 1992.
40. Balmain, A. Exploring the bowels of DNA methylation. Curr. Biol., *5:* 1013–1016, 1995.
41. Dietrich, W. F., Lander, E. S., Smith, J. S., Moser, A. R., Gould, K. A., Luongo, C., Borenstein, N., and Dove, W. F. Genetic identification of *Mom-1*, a major modifier locus affecting *Min*-induced intestinal neoplasia in the mouse. Cell, *75:* 631–639, 1993.
42. Donehower, L. A., Harvey, M., Slagle, B. L., McArthur, M. J., Montgomery Jr, C. A., Butel, J. S., and Bradley, A. Mice deficient for p53 are developmentally normal but susceptible to spontaneous tumors. Nature (Lond.), *356:* 215–221, 1992.
43. Sah, V. P., Attardi, L. D., Mulligan, G. J., Williams, B. O., Bronson, R. T. A subset of p53-deficient embryos exhibits exencephaly. Nat. Genet., *10:* 175–180, 1995.
44. Gould, K. A., Dietrich, W. F., Borenstein, N., Lander, E. S., and Dove, W. F. *Mom1* is a semi-dominant modifier of intestinal adenoma size and multiplicity in *Min*/+ mice. Genetics, *144:* 1769–1776, 1996.
45. Timme, T. L., and Thompson, T. C. Rapid allelotype analysis of *p53* knockout mice. BioTechniques, *17:* 460–463, 1994.
46. Potten, C. S., Li, Y. Q., O'Connor, P. J., and Winton, D. J. A possible explanation for the differential cancer incidence in the intestine, based on distribution of the cytotoxic effects of carcinogens in the murine large bowel. Carcinogenesis (Lond.), *13:* 2305–2312, 1992.
47. Potten, C. S., Roberts, S. A., Chwalinski, S., Loeffler, M., and Paulus, U. Scoring mitotic activity in longitudinal sections of crypts of the small intestine. Cell Tissue Kinet., *21:* 231–246, 1988.
48. Engle, S. J., Hoying, J. B., Boivin, G. P., Ormsby, I., Gartside, P. S., and Doetschman, T. Transforming growth factor β1 suppresses nonmetastatic colon cancer at an early stage of tumorigenesis. Cancer Res., *59:* 3379–3386, 1999.
49. Levine, A. J. p53, the cellular gatekeeper for growth and division. Cell, *88:* 323–331, 1997.
50. Halberg, R. B., Katzung, D. S., Hoff, P. D., Moser, A. R., Cole, C. E., Lubet, R. A., Donehower, L. A., Jacoby, R. F., and Dove, W. F. Tumorigenesis in the multiple intestinal neoplasia mouse: redundancy of negative regulators and specificity of modifiers. Proc. Natl. Acad. Sci. USA, *97:* 3461–3466, 2000.
51. Chuang, L. S-H., Ian, H., Koh, T-W., Ng, H-H., Xu, G., and Li, B. F. L. Human DNA-(cytosine-5) methyltransferase-PCNA complex as a target for p21^{WAF1}. Science (Washington DC), *26:* 1996–2000, 1997.
52. Fournel, M., Sapieha, P., Beaulieu, N., Besterman, J. M., and MacLeod, A. R. Down-regulation of human DNA-(cytosine-5) methyltransferase induces cell cycle regulators *p16*^{INK4a} and *p21*$^{WAF/Cip1}$ by distinct mechanisms. J. Biol. Chem., *274:* 24250–24256, 1999.
53. Deng, C., Zhang, P., Harper, J. W., Elledge, S. J., and Leder, P. Mice lacking p21$^{CIP1/WAF1}$ undergo normal development, but are defective in G_1 checkpoint control. Cell, *82:* 675–684, 1995.
54. Waldman, T., Kinzler, K. W., and Vogelstein, B. p21 is necessary for the p53-mediated G_1 arrest in human cancer cells. Cancer Res., *55:* 5187–5190, 1995.
55. Cormier, R. T., Hong, K. H., Halberg, R. B., Hawkins, T. L., Richardson, P., Mulherkar, R., Dove, W. F., and Lander, E. S. Secretory phospholipase Pla2g2a confers resistance to intestinal tumorigenesis. Nat. Genet., *17:* 88–91, 1997.
56. Beazer-Barclay, Y., Levy, D. B., Moser, A. R., Dove, W. F., Hamilton, S. R., Vogelstein, B., and Kinzler, K. W. Sulindac suppresses tumorigenesis in the Min mouse. Carcinogenesis (Lond.), *17:* 1757–1760, 1996.
57. Mahmoud, N. N., Boolbol, S. K., Dannenberg, A. J., Mestre, J. R., Bilinski, R. T., Martucci, C., Newmark, H. L., Chadburn, A., and Bertagnolli, M. M. The sulfide metabolite of sulindac prevents tumors and restores enterocyte apoptosis in a murine model of familial adenomatous polyposis. Carcinogenesis (Lond.), *19:* 87–91, 1998.
58. Mahmoud, N. N., Bilinski, R. T., Churchill, M. R., Edelmann, W., Kucherlapati, R., and Bertagnolli, M. M. Genotype-phenotype correlation in murine *Apc* mutation: differences in enterocyte migration and response to sulindac. Cancer Res., *59:* 353–359, 1999.
59. Mahmoud, N. N., Boolbol, S. K., Bilinski, R. T., Martucci, C., Chadburn, A., and Bertagnolli, M. M. *Apc* gene mutation is associated with a dominant-negative effect upon intestinal cell migration. Cancer Res., *57:* 5045–5050, 1997.
60. Lipkin, M., Blattner, W. E., Fraumeni, J. F., Lynch, H. T., Deschner, E., and Winawer, S. Tritiated thymidine (φ_p,φ_h) labeling distribution as a marker for hereditary predisposition to colon cancer. Cancer Res., *43:* 1899–1904, 1983.
61. Wasan, H. P., Park, H-S., Liu, K. C., Mandir, N. K., Winnett, A., Sasieni, P., Bodmer, W. F., Goodlad, R. A., and Wright, N. A. APC in the regulation of intestinal crypt fission. J. Pathol., *185:* 246–255, 1998.
62. Brunk, B. P., Goldhamer, D. J., and Emerson, Jr, C. P. Regulated demethylation of the *Myo*D distal enhancer during skeletal myogenesis. Dev. Biol., *177:* 490–503, 1996.
63. Szyf, M., Rouleau, J., Theberge, J., and Bozovic, V. Induction of myogenic differentiation by an expression vector encoding the DNA methyltransferase cDNA sequence in the antisense orientation. J. Biol. Chem., *267:* 12831–12836, 1992.
64. Bestor, T. H., Hellewell, S. B., and Ingram, V. M. Differentiation of two mouse cell lines is associated with hypomethylation of their genomes. Mol. Cell. Biol., *4:* 1800–1806, 1984.
65. Walsh, C. P., and Bestor, T. H. Cytosine methylation and mammalian development. Genes Dev., *13:* 26–34, 1999.
66. Ramchandani, S., Bhattacharya, S. K., Cervoni, N., and Szyf, M. DNA methylation is a reversible biological signal. Proc. Natl. Acad. Sci. USA, *96:* 6107–6112, 1999.
67. Kanai, Y., Ushijima, S., Nakanishi, Y., and Hirohashi, S. Reduced mRNA expression of the DNA demethylase, MBD2, in human colorectal and stomach cancers. Biochem. Biophys. Res. Commun., *264:* 962–966, 1999.
68. Shoemaker, A. R., Moser, A. R., and Dove, W. F. *N*-ethyl-*N*-nitrosourea treatment of multiple intestinal neoplasia (Min) mice: age-related effects on the formation of intestinal adenomas, cystic crypts, and epidermoid cysts. Cancer Res., *55:* 4479–4485, 1995.
69. Toyota, M., Ahuja, N., Ohe-Toyota, M., Herman, J. G., Baylin, S. B., and Issa, J-P. J. CpG island methylator phenotype in colorectal cancer. Proc. Natl. Acad. Sci. USA, *96:* 8681–8686, 1999.
70. De Marzo, A. M., Marchi, V. L., Yang, E. S., Veeraswamy, R., Lin, X., and Nelson, W. G. Abnormal regulation of DNA methyltransferase expression during colorectal carcinogenesis. Cancer Res., *59:* 3855–3860, 1999.
71. Eads, C. A., Danenberg, K. D., Kawakami, K., Saltz, L. B., Danenberg, P. V., and Laird, P. W. CpG island hypermethylation in human colorectal tumors is not associated with DNA methyltransferase overexpression. Cancer Res., *59:* 2302–2306, 1999.